Reports on Geodesy and Geoinformatics, 2025, Vol. 120, pp. 109–119

DOI: 10.2478/rgg-2025-0022
Received: 27 November 2025 / Accepted: 19 December 2025
Published online: 23 December 2025

ORIGINAL ARTICLE

3D Building documentation using portable LiDAR systems – functionality analysis

Kinga Wawrzyniak [1*], Maria Elżbieta Kowalska [2], Janina Zaczek-Peplinska [2] and Zbigniew Muszyński [1]

[1]Faculty of Geoengineering, Mining and Geology, Wrocław University of Science and Technology, Wybrzeże Stanisława Wyspiańskiego 27, 50-370 Wrocław, Poland
[2]Faculty of Geodesy and Cartography, Warsaw University of Technology, 1 Politechniki Square, 00-661 Warsaw, Poland

*kinga.wawrzyniak@pwr.edu.pl

Abstract

Contemporary building documentation increasingly relies on laser scanning technologies that provide rapid and precise spatial data acquisition. Portable LiDAR systems such as the Leica BLK360, as well as mobile devices like the iPad, offer modern tools for efficient documentation of interior spaces, including office rooms. With dedicated applications (e.g., Leica Cyclone Field 360, Leica Cyclone 3DR, MagicPlan, BIMx, AutoCAD Mobile), users can record measurements, create sketches, and generate 3D models and photographic documentation within a single digital environment. The purpose of this study is to assess the dimensional accuracy in the documentation of an office space using portable LiDAR systems. The experiments showed that, for most analysed dimensions, the results agreed within several centimetres, which is sufficient for architectural inventory work. However, the issue of rounded corners was identified, which may significantly influence measurement results depending on the distance-measurement method applied. Reliable accuracy analysis required proper mutual alignment (common georeferencing) of the scans acquired with the selected instruments. To achieve this, point cloud classification was performed to identify surfaces suitable for cloud-to-cloud alignment. A predefined AI-based classification model dedicated to indoor environments was used. The findings confirm that portable LiDAR systems significantly reduce the time required to complete inventory tasks and enable more comprehensive visualisation of interior spaces. This technology serves as an effective tool supporting the design, modernisation, and management of office environments in a digital workflow, although its accuracy-related limitations must be considered.

Key words: 3D building inventory, terrestrial laser scanning, point cloud accuracy, low-cost laser scanning, portable LiDAR devices

1 Introduction

Inventory of a premises, as defined in Polish construction law, is a technical documentation that describes its actual condition. It must be prepared by a person holding the appropriate professional qualifications (Art. 12(2) of the Construction Law (1994)) and typically includes floor plans, sections, elevations, a technical description, and photographic records. Such documentation is essential for producing accurate technical drawings required for renovations, modernisation projects, architectural design, property sales, or the legalisation of unauthorised construction. The inventory enables precise determination of room dimensions, the location of installations (electrical, plumbing, heating), and other fixed elements, which is crucial for planning work and assessing the technical condition of the property. In Poland, inventories of residential premises are prepared in compliance with the PN-ISO 9836:2022-07 (2022) standard, which replaced the earlier 1997 and 2015 versions. Under current regulations, this standard is mandatory when calculating the floor area of single-family houses and residential units.

A distinct area of inventory work concerns office spaces, allowing assessment of individual workstation compliance with occupational health and safety requirements and ergonomic standards.

According to the Regulation of the Minister of Labour and Social Policy on occupational health and safety, each employee working simultaneously in an office space must be provided with at least 13 m^3 of free room volume and at least 2 m^2 of free floor area not occupied by equipment or furnishings. If an employee works in the room for more than four hours per day, the height of the space may not be less than 3 m.

Modern, easy-to-use measurement instruments – such as the Z+F Imager 5006h terrestrial laser scanner, the BLK360, and portable LiDAR solutions (e.g., the iPad or iPhone 13 Pro LiDAR) – enable efficient surveying of both empty spaces and rooms filled with furniture and documentation. Portable LiDAR systems are widely used in building documentation (BIM, architectural surveys, renovation projects) (Mêda et al., 2023), technical installation inventories, documentation of outdoor infrastructure (sidewalks, roads, cycle paths, poles, utility boxes, hydrants, signs, barriers) (Saptari et al., 2024), green-space and environmental surveys (Gollob et al., 2021; Krausková et al., 2025; Tatsumi et al., 2022), heritage architecture documentation (Ulvi and Hamal, 2025), industrial inventories, surveys of hard-to-reach structures (utility ducts, caves) (Ordóñez et al., 2024), and in the assessment of damage following emergency events (Guerriero et al., 2024; Kottner et al., 2023). Like other scanning technologies, portable LiDAR solutions are defined by their accuracy and resolution, mobility and operating speed, as well as the overall completeness and quality of the acquired data, all of which must be considered in relation to the cost of the chosen method (Atencio et al., 2024).

Portable LiDAR systems offer a flexible solution for rapid, mobile measurements, interior surveys, and applications where accessibility is critical. Traditional TLS instruments, in turn, provide the highest data quality, better accuracy, and denser point clouds, which are essential for precise modelling and detailed technical documentation. Across multiple projects, the most effective results can be achieved by combining both technologies, as confirmed by the findings of this article.

This study compares the basic parameters of the instruments, evaluates their accuracy, and assesses their functionality in the context of inventory applications. For tasks related to floor-plan redevelopment, changes in equipment layout, and the placement of new electrical or network access points, the following point-cloud characteristics were identified and compared as particularly relevant: accuracy, range, and the ease of supplementing identified data gaps. Within the available manufacturer-provided software (bundled with the devices or accessible online), the ease of automatic point cloud classification and the use of its results to assess room utilisation were also evaluated.

The analyses presented in this article draw on widely used methods for assessing point clouds in terms of their level of detail and completeness. Completeness refers to how fully and accurately a point cloud reflects the actual geometry of an object or scene – that is, whether all parts of the surface have been captured and whether gaps or shadow zones are absent. The literature offers numerous approaches to point-cloud assessment (Fretes et al., 2019; Javaheri et al., 2017; Rizali et al., 2022; Zhuang et al., 2024), including point-based analysis, line-based analysis, geometry fitting, cross-section analysis, and global point-cloud assessment. In global analyses, quality assessment does not focus on individual measurement points alone but also considers the spatial neighbourhood within a defined radius. Such evaluation may be performed visually – by examining the correctness of recorded intensity or colour, the fidelity of shape representation, and the overall completeness of the point cloud – or analytically, by assessing point-cloud density, grid regularity, or variations in normal vectors. In this study, both point-based and visual assessments were used to evaluate the quality of pairwise registration, georeferencing, and classification of the acquired point clouds. The consistency of the integrated datasets from the terrestrial laser scanner and the portable LiDAR system was also examined. Furthermore, quantitative analyses were conducted to evaluate the accuracy of captured dimensions and edge extraction in the context of documenting an office interior.

Figure 1. View of the office space that is the subject of further analysis

2 Materials and methods

2.1 Research object

A 24.6 m^2 office room located on the third floor of the Main Building of the Warsaw University of Technology served as the study area. The room contained one large window, two desks with chairs, two spacious cabinets, and assorted smaller office items (Figure 1).

2.2 Description of the scanners

For the analysis, three scanning devices were used, differing in measurement technology, accuracy, and purchase cost:

- The phase-based Z+F Imager 5006h
- The pulsed Leica BLK360 (used in two modes: standalone BLK360 scanning and a gap-filling mode supported by an iPad Pro 11 M4 equipped with LiDAR)
- The iPhone 13 Pro LiDAR

The basic technical specifications of the instruments are presented in Table 1.

2.3 Description of the measurements

The phase-based Z+F Imager 5006h scanner was used to survey the test room from two instrument positions. The following parameters were applied: resolution = superhigh, quality = normal, laser mode = normal. As this device offers the highest measurement accuracy among all instruments considered (according to the manufacturer's specifications), the resulting point cloud is treated as the reference dataset and is denoted as "Z+F" (Table 1).

The Leica BLK360 pulsed scanner was used from two positions corresponding to those of the Z+F Imager 5006h. The measurement parameters were resolution = Dense+ (4 mm at 10 m), photo mode = HDR, with GNSS positioning disabled. The resulting point cloud is denoted as "BLK" (Table 1).

The BLK360 is operated via a tablet running the Leica Cyclone Field 360 application. Some higher-end tablets – such as the iPad Pro 11 M4 used in this study – are equipped with LiDAR-based environmental scanning. In such cases, data collected by the BLK360 can be supplemented with a much sparser point cloud captured directly by the tablet. Tablet-based scanning serves to fill gaps in the BLK360 cloud in areas inaccessible to the scanner. These tablet-scanned fragments are assigned to the appropriate scanner positions as tags and automatically merged with the point cloud

Table 1. Characteristics of the measuring instruments used

Measuring instrument	Data-set name	Scanning resolution	Field of view	Point-measurement rate	Range	Cost
Z+F Imager 5006h	Z+F	0.3 mm per 10 m	360° (horizontal) / 310° (vertical)	1 020 000 pts/sek.	up to 79 m	high cost
BLK360	BLK	4 mm per 10 m	360° (horizontal) / 270° (vertical)	680 000 pts/sek.	up to 45 m	medium cost
BLK360 + iPad Pro 11 M4*	BLK+iPad	4 mm per 10 m	360° (horizontal) / 270° (vertical)	680 000 pts/sek.	up to 45 m	medium cost
iPhone13 Pro LiDAR	iPhone	10-20 mm per 2 m	120° (horizontal) / 30° (vertical)	no data	up to 5 m	low cost

* No resolution or scanning-accuracy data for the iPad Pro 11 M4 are provided in the manufacturer's documentation.

from each scanner position. In this experiment, supplementary tablet scans were performed for both scanner setups to cover areas outside the scanner's line of sight. The integrated dataset combining BLK360 and iPad Pro 11 M4 measurements is denoted as "BLK+iPad" (Table 1).

The iPhone 13 Pro LiDAR was used in a manner analogous to terrestrial laser scanning: at each measurement position, the operator remained stationary and rotated 360° while holding the device. Three measurement positions were used. Scanning was performed with the following parameters: iPhone 13 Pro LiDAR with the 3D Scanner App (Laan Labs, New York, USA), High Resolution mode, max depth = 5 m, resolution = 10 mm, confidence = high, masking = off. The 3D Scanner App for Mac is a desktop tool that uses photogrammetry via the Object Capture API to process photos and videos into 3D models on supported hardware. The point cloud obtained with the iPhone 13 Pro LiDAR is denoted as "iPhone" (Table 1).

2.4 Classification of point clouds

All four datasets (Z+F, BLK, BLK+iPad, iPhone) were subjected to automatic classification using Cyclone 3DR software. The predefined AI-based Indoor 2.2 model, designed specifically for indoor environments, was applied. The procedure produced a total of 27 classes, although some appeared only in selected datasets. Several classes also contained a small number of points or included points that had been incorrectly assigned. Therefore, a subsequent manual classification step was conducted to correct misclassified portions of the point clouds.

2.5 Georeferencing of point clouds

A unified georeferencing procedure for all datasets was conducted in RiSCAN Pro software. The workflow consisted of the following steps:

a) For each dataset, all classes were imported except those classified as measurement noise (e.g., false reflections from the window glass).
b) An additional class named *Hard_surf* was created to represent permanent room elements considered stable over time and characterised by favourable laser-reflection properties. This class included points originally assigned to Wall, Floor, and Ceiling, as well as part of the cabinet surfaces treated as stationary.
c) A coarse registration was performed by aligning the BLK, BLK+iPad, and iPhone clouds to the coordinate system of the Z+F dataset, which served as the reference. Five manually selected point pairs were used for this initial alignment.
d) For each dataset, automatic plane detection was performed on points belonging to the *Hard_surf* class using the following parameters:
   - Minimum number of points per plane: 30
   - Maximum plane error: 0.020 m
   - Minimum search cube size: 0.064 m
   - Maximum search cube size: 2.048 m
e) The final georeferencing of the point clouds was obtained by mutually adjusting the datasets using the detected planes and applying robust estimation to minimise the influence of noise and device-related measurement inaccuracies. The computations were performed in the *MultiStation Adjustment* module of RiSCAN Pro software with the following parameters:
   - All nearest points used for search
   - Search radius: 0.05 m
   - Maximum tilt angle: 5°

For the reference cloud (Z+F dataset), rotation, translation, and scale were fixed. The remaining datasets were adjusted with six degrees of freedom, except for scale, as each instrument was assumed to record the correct scale during measurement.

2.6 Distance measurement methodology

To assess how the choice of scanner affects both the accuracy of the reconstructed geometry and the consistency of the derived room dimensions, a series of distance measurements was performed in Autodesk ReCap software according to the scheme shown in Figure 2. Distances were measured orthogonally using local reference planes fitted to selected wall or recess segments, ensuring consistent and repeatable measurements across all four datasets. However, not all dimensions could be derived from every dataset. In the Z+F and iPhone datasets, the window recess was obscured by a lowered blind, while in the BLK and BLK+iPad datasets, the entrance door was closed, preventing measurement of the door recess.

2.7 Consistency assessment of the BLK+iPad dataset

The automatic integration of a high-resolution, geometrically consistent BLK360 point cloud with additional tablet-based scans raises questions about the geometric consistency of such a hybrid dataset. The tablet's sensor is inherently less accurate, and the user has no control over the quality of the automated merging process. If low-quality regions are identified, tablet-scanned fragments (tags) can be manually disabled.

To evaluate the actual accuracy of the BLK+iPad combination, two regions within the BLK+iPad cloud were analysed, specifically the floor fragments located beneath the scanner tripod at both positions. At the first scanner position, the gap in the point cloud

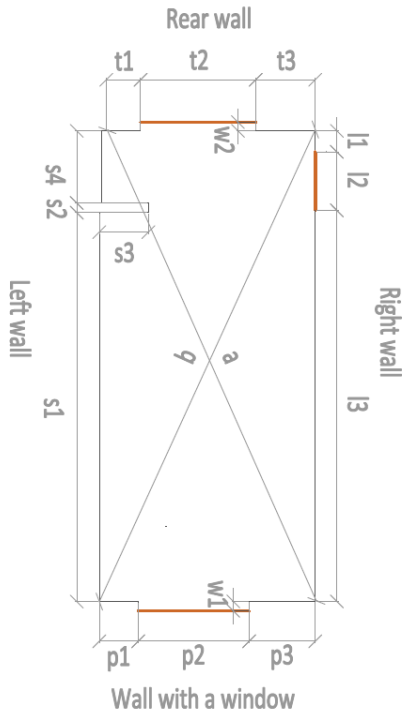

Figure 2. Room-dimension labels

was filled with a single tablet scan assigned as one tag. At the second position, the gap was filled with two overlapping tablet scans, assigned as two separate tags. A dense BLK360 point cloud representing the surrounding floor (outside the tripod shadow) was used to fit a plane that filled the missing region in the dense cloud. This plane served as the reference surface for assessing the tablet-scanned points, which ideally should coincide with it. Geometric consistency deviations were computed as the vertical distances between the tablet-acquired points and the reference plane.

3 Results

3.1 Registration results for the point clouds

The point clouds acquired from the two Z+F Imager 5006h scanner positions were registered in a common coordinate system using black-and-white reference targets affixed to the walls and furniture.

After completing the Leica BLK360 measurements, the data were exported and registered in a common coordinate system using the same reference targets together with cloud-to-cloud alignment. Registration of the BLK dataset was performed in Cyclone Register360 software, yielding:

- Total link error between two stations: 0.0015 m
- Mean target error: 0.0017 m
- Cloud-to-cloud error: 0.0013 m
- Overlapping of two point clouds: 77%
- Strength parameter: 60%

The strength parameter reflects how strongly the surface correspondences constrain the remaining degrees of freedom in the overlapping regions of the two point clouds. It is assessed in planes perpendicular to the axes of the adopted Cartesian coordinate system, and its final value corresponds to the percentage of overlap in the weakest-represented plane.

The merged point clouds (BLK360 scans supplemented with iPad Pro 11 M4 measurements) were processed analogously. Registration of the BLK+iPad dataset in Cyclone Register360 produced:

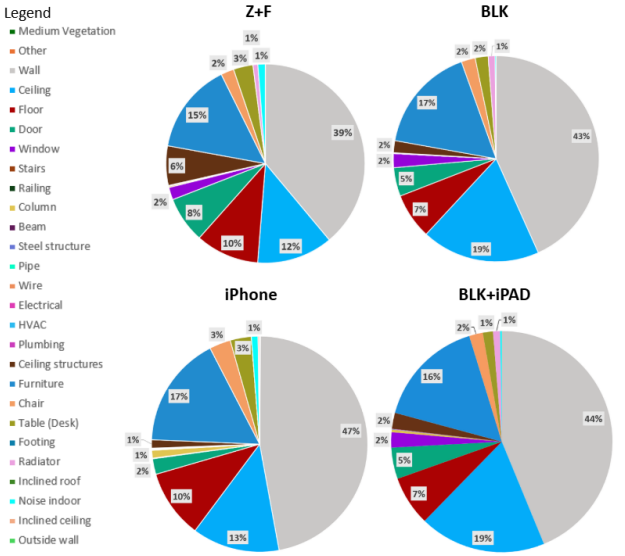

Figure 3. Percentage distribution of points across classes for the analysed datasets

- Total link error between two stations: 0.0017 m
- Mean target error: 0.0020 m
- Cloud-to-cloud error: 0.0015 m
- Overlapping of two point clouds: 82%
- Strength parameter: 63%

For the iPhone dataset, standard registration-accuracy metrics are not available. The geometric accuracy of this point cloud is assessed later in the article based on the room-dimension comparison.

3.2 Classification results

Automatic classification produced distinct sets of classes for each dataset. In total, 27 classes were identified, although some contained a limited number of points, as shown in Figure 3.

The results show clear variation in the proportion of points assigned to the largest classes depending on the measurement device. For the Wall class, the following values were obtained: Z+F 39%, BLK 43%, BLK+iPad 44%, and iPhone 47%. For the Floor class: Z+F 10%, BLK 7%, BLK+iPad 7%, and iPhone 10%. For the Ceiling class: Z+F 12%, BLK 19%, BLK+iPad 19%, and iPhone 13%. The greatest divergence – nearly 10% – occurred in the Wall class, while the closest agreement was observed for the Floor class. Combining the iPad with the BLK scanner did not significantly alter the results compared to using the BLK alone.

Visual inspection of the automatic classification revealed local errors, particularly within the Wall, Door, and Furniture classes. Figure 4a shows incomplete extraction of the door (green colour), while Figure 4b shows a cabinet misclassified as Wall (grey colour). Floor-classification errors are visible in Figure 4d (blue colour). With high-quality point clouds, it was also possible to identify the radiator and associated piping (Figure 4c). As noted earlier, manual correction was applied to adjust misclassified points, with particular attention to classes relevant for cloud-to-cloud georeferencing.

The automatic classification outputs can be effectively used to assess available free floor area for employees, supporting interior inventory tasks required to verify compliance with occupational health and safety regulations. In Figure 4d, the unoccupied floor areas – free of furniture and other equipment – are evident.

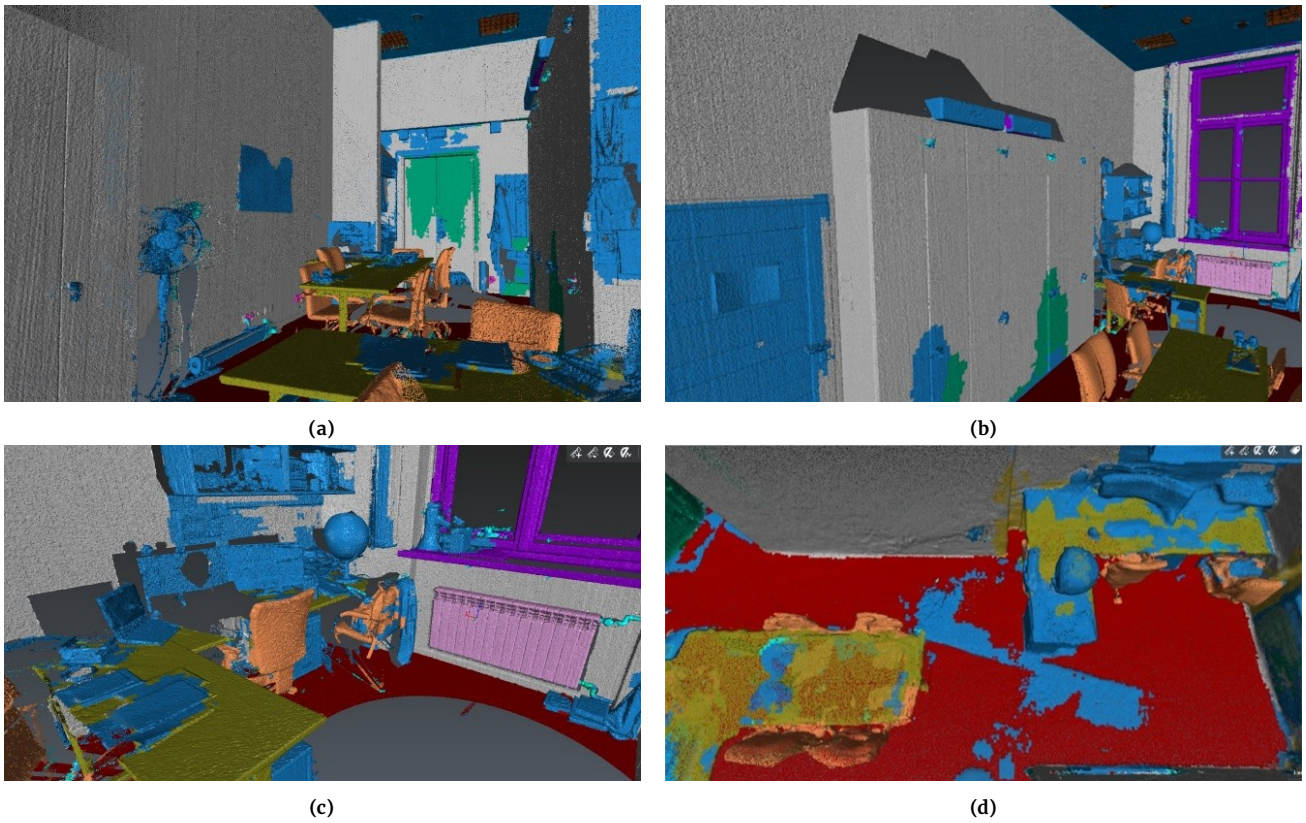

Figure 4. Point cloud after automatic classification for: (a) BLK, (b) BLK, (c) BLK, (d) iPhone. Grey denotes the Wall, green the Door, blue the Furniture, and red the Floor

3.3 Results of georeferencing the point clouds

The results of automatic plane detection within the *Hard_surf* class are shown in Figure 5. The relatively sparse, low-noise point cloud acquired with the Z+F scanner produced fewer planes with larger spatial extent Figure 5a. In contrast, the much denser BLK point cloud (Figure 5b) exhibits slightly higher measurement noise. As a result, its high spatial resolution and the variability of local normal vectors led to the identification of a substantially larger number of planes, each with a smaller surface area. Incorporating the tablet-derived points (Figure 5c) did not substantially alter the overall plane distribution, although it introduced several new planes in areas that were previously empty, such as under the tripod positions. For the iPhone dataset, difficulties in defining the boundaries of the detected planes are evident. This is particularly noticeable along the wall-ceiling junction (Figure 5d), where plane edges appear irregular and do not form clear, continuous boundaries.

The detected planes were subsequently used for georeferencing the point clouds via robust estimation. An example of plane-based alignment between the Z+F reference cloud (orange) and the transformed BLK cloud (blue) is presented in Figure 6.

Residual histograms for the BLK, BLK+iPad, and iPhone datasets relative to the Z+F reference cloud are shown in Figure 7. The BLK dataset achieved the highest alignment accuracy, with a standard deviation of 0.7 mm and a quite regular shape of the histogram (Figure 7a). For the BLK+iPad cloud, the standard deviation was remarkably similar (0.8 mm), although the histogram shape showed slightly greater irregularity (Figure 7b). A pronounced decrease in accuracy occurred for the iPhone dataset, where the standard deviation reached 11.8 mm and the histogram shape was close to bimodal (Figure 7c).

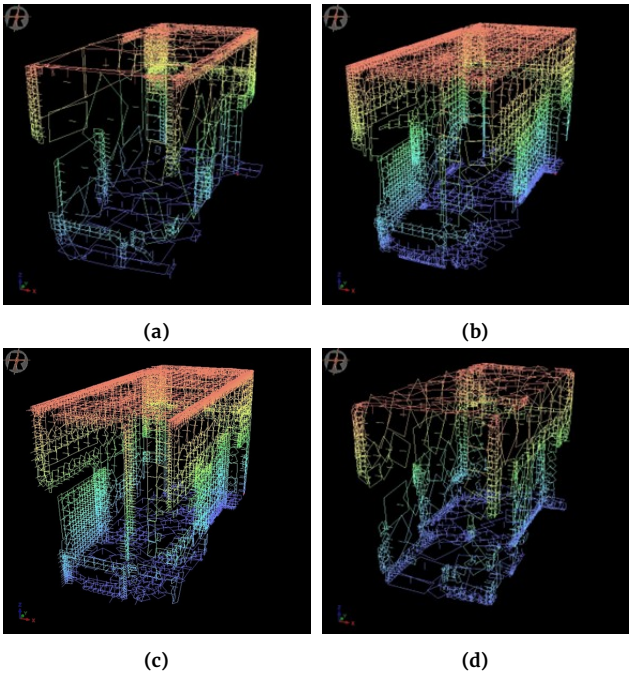

Figure 5. Visualisation of planes detected within the *Hard_surf* class for: (a) Z+F, (b) BLK, (c) BLK+iPad, (d) iPhone

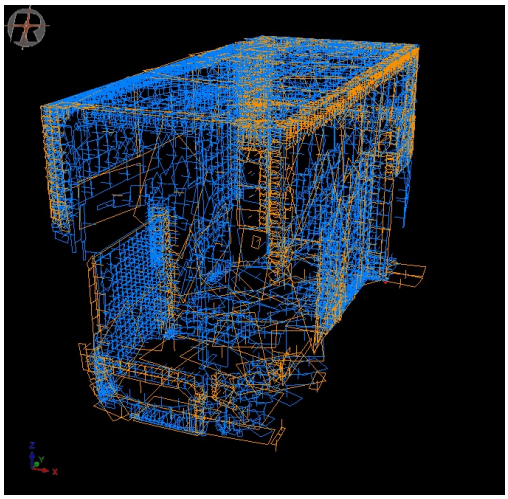

Figure 6. Quality check of point-cloud alignment after georeferencing: orange – Z+F dataset as the reference; blue – BLK dataset after transformation

3.4 Distance-measurement results

The results of the distance measurements are presented in Table 2. The smallest discrepancies in distance measurements were observed between the BLK+iPad and Z+F datasets, even though the BLK360 is a lower-class scanner compared with the Z+F 5006h. Standard deviations of differences between distances measured from other equipment and Z+F data (treated as a reference value) are presented in Table 2. For BLK and BLK+iPad data, the values of standard deviations are remarkably similar (0.007 m and 0.006 m). These findings indicate that, for short distances, modern compact scanners can achieve accuracy comparable to high-precision instruments. The measurements obtained with the iPhone 13 Pro LiDAR show the greatest discrepancies from results produced by the other instruments. Dimensional differences ranged from a few millimetres to several centimetres, especially when measuring more complex elements, such as window or door recesses. The largest differences occur in the diagonal measurements, reaching −94 mm, which reflects the limited ability of the iPhone 13 Pro LiDAR to accurately reconstruct room edges. The standard deviation of all dimensional differences between the iPhone data and the Z+F data was 0.044 m.

The accuracy of the room-dimension measurements depends on how precisely individual elements of the room are represented in the point cloud. Here, precision is understood as the degree of corner rounding. The analysed datasets revealed substantial variation in this respect, as shown in Figure 8.

The accuracy of corner reconstruction depends on both the scanner's measurement noise and the resolution of the point cloud. The Z+F and BLK datasets provide the most faithful representation of corner geometry. The greatest corner rounding was observed in the iPhone data, reaching several centimetres in each corner, which corresponds to the nearly 10-centimetre differences in diagonal lengths compared with the other scanning techniques (Figure 9). In the BLK data, a characteristically thicker point-cloud layer is visible, which affects the accuracy of geometric attributes such as surface flatness. This increased thickness is caused by measurement noise, which is considerably less pronounced in the phase-based Z+F Imager 5006h.

In the BLK+iPad data, an additional increase in point-cloud thickness is visible, caused by the inclusion of tablet-acquired points. This analysis highlights distinct differences in point-cloud quality. This aspect is crucial when selecting a measurement technology, as similar rounding effects will also appear in other architectural elements, such as window and door openings or interior furnishings.

3.5 Consistency assessment of the BLK+iPad dataset

A clear difference between the density of the BLK point cloud (Dense+ mode) and the density of the tablet-acquired gap-filling points is visible in Figure 10a. The geometric consistency assessment shows flatness deviations of up to +9 mm for the tablet-derived points relative to the dense BLK360 surroundings (Figure 10b). At the second scanner position, the tripod shadow was filled with two overlapping tablet scans (Figure 11a). Consequently, two separate layers of points were generated, each representing the floor surface but not coinciding with one another. The lower layer (Figure 11b) lies below the actual floor level, with flatness deviations reaching −11.5 mm; for 48.6% of the filled area, the deviations range from −10.1 mm to −8.6 mm. The upper layer (Figure 11c) lies above the actual floor level, with deviations as high as +31.7 mm; for 24% of the area, the deviations fall within the range of +19.8 mm to +23.8 mm.

4 Discussion

The accuracy of modern terrestrial (TLS) and mobile (Mobile 3D Scanner) laser scanners enables their use across a wide range of geodetic and construction applications, including the detection of deformation in metro tunnels (Feng et al., 2025), monitoring static load tests on foundation piles (Muszyński and Rybak, 2021), and assessing the roughness of geotechnical structures (Wyjadłowski et al., 2021). In architecture, laser scanners are widely used for modelling and documenting heritage sites (Martinenko et al., 2025) and for generating digital representations of objects in virtual-reality environments – so-called Digital Twins (Clini et al., 2025). Despite these advantages, the high cost of professional laser scanners remains a barrier to broader adoption. At the same time, the availability of far cheaper tablets and smartphones equipped with LiDAR sensors has encouraged attempts to replace professional scanners with less specialised measuring devices. This gives rise to an important question: what is the acceptable balance between cost and the quality of the resulting point clouds? In the relevant literature, numerous publications attempt to use cheaper solutions to obtain three-dimensional models in the form of point clouds (Sirmacek and Lindenbergh, 2014). In 2020, Apple Inc. released the first phone with innovative built-in LiDAR (Light Detection and Ranging) depth sensors and an enhanced augmented reality (AR) application programming interface (API). The introduction of phones with built-in LiDAR by Apple represents a kind of breakthrough in access to affordable scanning solutions. In the work Vogt et al. (2021), authors undertook an evaluation of the accuracy of scanning multi-coloured Lego bricks with the iPad Pro. The results they obtained showed that LiDAR technology is impractical for scanning small objects, such as Lego bricks. The authors noted that LiDAR depth data is combined with accompanying colour (RGB) data using artificial intelligence to create a depth map. Furthermore, the depth map grid consists of triangles with large faces, which means that LiDAR can be used to support augmented reality or to scan large objects, such as rooms, but it is not suitable for scanning small objects. Similar conclusions were drawn by authors who attempted to use Apple devices for tasks requiring much less precision, such as forest measurements (Mokroš et al., 2021) or geomorphological forms (Riquelme et al., 2021). Despite certain limitations, from the very beginning, the authors of the publications have pointed out the enormous potential of this technology (Abbas and Abed, 2024; Teppati Losè et al., 2022). It should also be emphasised that this technology is developing rapidly, which is evident both in terms of software development and the increasingly better results of studies conducted using portable LiDAR systems.

Table 2. Room-dimension measurement results and differences between distances measured from other equipment and Z+F data (treated as a reference value), as well as the standard deviation of these differences

Wall label	Dimension label	Z+F (dist.)	iPhone (dist.)	Differ. (iPhone vs. Z+F)	BLK (dist.)	Differ. (BLK vs. Z+F)	BLK+iPad (dist.)	Differ. (BLK+iPad vs. Z+F)
Wall with a window	p1 [m]	–	–	–	0.605	–	0.604	–
	p2 [m]	–	–	–	1.720	–	1.719	–
	p3 [m]	–	–	–	1.037	–	1.037	–
	p1+p2+p3 [m]	3.362	3.367	0.005	3.362	0.000	3.360	-0.002
Left wall	s1 [m]	6.050	6.031	-0.019	6.049	-0.001	6.050	0.000
	s2 [m]	0.147	0.134	-0.013	0.150	0.003	0.154	0.007
	s3 [m]	0.749	0.769	0.020	0.762	0.013	0.753	0.004
	s4 [m]	1.129	1.130	0.001	1.129	0.000	1.130	0.001
Rear wall	t1 [m]	0.698	0.696	-0.002	0.689	-0.009	0.691	-0.007
	t2 [m]	1.302	1.298	-0.004	1.306	0.004	1.306	0.004
	t3 [m]	1.237	1.209	-0.028	1.231	-0.006	1.234	-0.003
Right wall	l1 [m]	0.365	0.419	0.054	–	–	–	–
	l2 [m]	0.902	0.946	0.044	–	–	–	–
	l3 [m]	6.074	6.013	-0.061	–	–	–	–
	l1+l2+l3 [m]	7.341	7.378	0.037	7.335	-0.006	7.339	-0.002
Recesses	w1 [m]	–	–	–	0.189	–	0.186	–
	w2 [m]	0.114	0.090	-0.024	0.110	-0.004	0.110	-0.004
Diagonals	a [m]	7.983	7.897	-0.086	7.997	0.014	7.995	0.012
	b [m]	8.062	7.968	-0.094	8.067	0.005	8.071	0.009
Standard deviation of differences		–	–	**0.044**	–	**0.007**	–	**0.006**

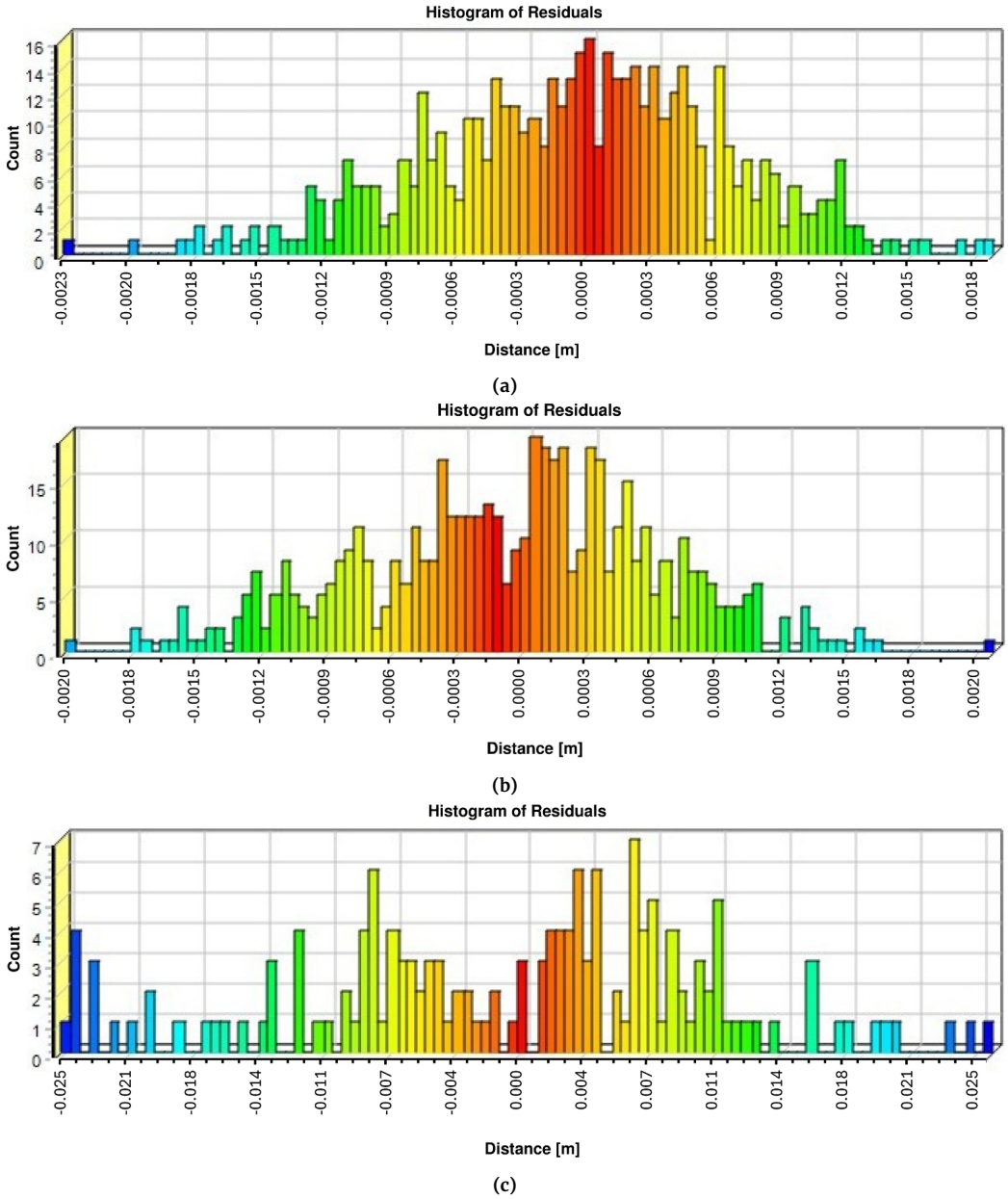

Figure 7. Residual histograms for the: (a) BLK, (b) BLK+iPad, and (c) iPhone datasets relative to the Z+F reference cloud

The suitability of LiDAR-equipped tablets for creating BIM models of cultural-heritage objects has been explored, for example, by Caffarri et al. (2025). The research presented in this paper focuses on evaluating the accuracy of dimension reconstruction, as well as the classification of furnishings and the surface characteristics of walls and interior elements, in the context of contemporary office spaces.

The results confirm that the differences between data acquired with high-precision scanners and compact devices are small, typically within a range of a few millimetres, demonstrating that newer mobile devices can also provide high-quality geometric reconstruction. The largest deviations were recorded for the iPhone 13 Pro LiDAR, particularly in areas with complex geometry and along edges, which reflects the nature of its measurement method based on analysing and discretising the captured image. The issue of edge-reconstruction precision is also highlighted in other studies (Vogt et al., 2021), where the authors draw attention not only to geometric factors but also to the influence of surface colour on the results of iPad-based scanning. Similar observations were reported by Zaczek-Peplinska and Kowalska (2022), where differences between iPhone-derived dimensions and those obtained using a Z+F scanner reached 2–4 cm, with edge deformation identified as the main source of error. Despite these limitations, deviations of several centimetres remain acceptable for most architectural and construction inventory tasks, as well as for spatial assessments performed for occupational health and safety (BHP) purposes. This confirms the suitability of mobile scanners for less demanding applications. Both our previous findings (Zaczek-Peplinska and Kowalska, 2022) and the room-measurement results presented in Table 2 are consistent and indicate reduced measurement accuracy for dimensions of more complex elements, such as recesses or diagonals. The lower accuracy of corner-to-corner measurements (e.g., room diagonals) also stems from the corner-rounding effects illustrated in Figure 8 and Figure 9.

Particular attention should be paid to the method for assigning a common georeference to all analysed datasets, described in Section 2.5. This procedure relied on stable, time-invariant room elements that had been classified into a shared layer (*Hard_surf*). The common georeference was obtained by aligning planes automatically detected within this layer. High georeferencing accuracy

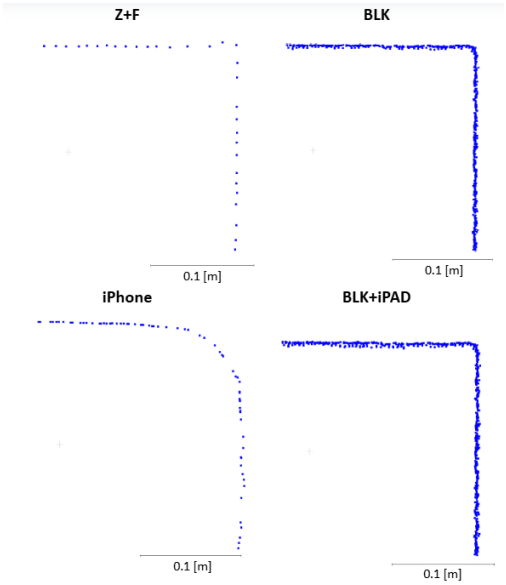

Figure 8. Views of the room corner for each point cloud

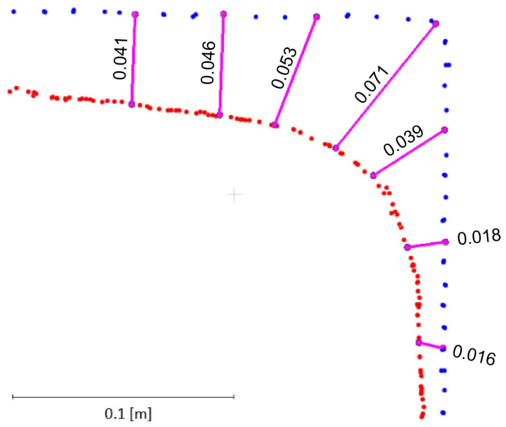

Figure 9. Results of spatial distance [m] measurements between room corners from two point clouds: red – iPhone data, blue – Z+F data

was achieved relative to the Z+F reference cloud, considered the dataset of highest precision and quality. For the iPhone data, the mean accuracy of 11.8 mm is a satisfactory result and meets typical requirements for architectural surveys. Achieving fitting accuracy on the order of 1 cm for all four datasets is particularly valuable when producing floor plans. Similar levels of accuracy have been reported by Caffarri et al. (2025), confirming the validity of the adopted point-cloud processing workflow. The authors plan to continue research for more complex spaces, such as long corridors, as well as buildings with multiple floors and rooms. It should be assumed that measurements of such large objects will require the establishment of a precise network of control points. An interesting issue will also be to check the workflow described in this article in the co-working office environments, which are increasingly common in contemporary business activities.

Automatic classification using artificial-intelligence algorithms streamlines and accelerates the extraction of characteristic interior elements, although some manual adjustments are sometimes necessary. The effectiveness of the classification depends strongly on the quality and density of the point clouds. High-resolution clouds allow for the correct detection of small components, such as the radiator pipe connections visible in the BLK (Figure 4c) and BLK+iPad datasets. Increased measurement noise, however, leads to classification errors – for example, furniture incorrectly identified on the floor in the iPhone dataset (Figure 4d). The quality of classification is important when using selected classes for georeferencing of point clouds. The resulting classification can also be used to automatically calculate the floor area occupied by office furniture, enabling the determination of the amount of free space per employee and, consequently, the verification of compliance with occupational health and safety requirements. Before calculating the occupied or unoccupied area, it is necessary to check the classification results. In the case described in the article, classification errors were indicated in the floor area. These errors can be assessed "visually" based on the colour assigned to the class without the need for in-depth analysis. Determining the surface for the purpose of assessing occupied or unoccupied areas does not require high accuracy of classification.

The quality of data acquired with portable LiDAR systems depends strongly on the scanning technique. In Atencio et al. (2024), the authors point out that the most important parameters to consider when planning a survey are a short object-to-sensor distance, a high scanning speed, and natural lighting conditions. They also note that iPad-based scanning exhibits reduced accuracy when capturing complex geometries or fine details in intricate heritage structures, a finding that aligns with the conclusions presented in this article.

The BLK+iPad cloud – BLK data supplemented with iPad measurements – offers sufficient accuracy for most room-dimensioning tasks involved in interior inventory work. iPad-based scanning helps reduce gaps in the point cloud; however, it is advisable to keep the tablet as close as possible to the areas being supplemented and to avoid duplicate scans. It is also useful to identify which scanner position is closest to the regions requiring completion and to assign the tablet-acquired data (tag) to that position. The discrepancy in cloud expansion may also result from the merging of two plane scans. One can assume that if the object were more spatially diverse, the match would be better.

5 Summary

The conclusions drawn from the literature review and from the comparison of data acquired with three scanning devices – Z+F Imager 5006h, BLK360, and the iPhone 13 Pro LiDAR – indicate that all three can be used for interior inventory surveys, provided that the recommendations outlined earlier are followed. The proposed point-cloud processing workflow – measurement, classification, and georeferencing – was tested and produced satisfactory results.

The measurement accuracies obtained for devices from different price ranges (the economically priced BLK360 and the low-cost iPhone 13 Pro LiDAR) can be regarded as reliable within 1–4 cm when compared with the reference data obtained from the professional and most expensive scanner in the group, the Z+F Imager 5006h. This level of accuracy is sufficient for measurements and analyses required for office-space valuation and for ensuring appropriate working conditions.

The results of the inventory measurements and the accuracy assessments of point clouds acquired using devices that differ in size, LiDAR technology, cost, and ease of use demonstrate the strong potential of more affordable solutions – such as the BLK360 and LiDAR-enabled iPhones – for building documentation. Nevertheless, the authors emphasise that smartphone-based scanning cannot replace precision methods based on terrestrial laser scanning or traditional geodetic surveying.

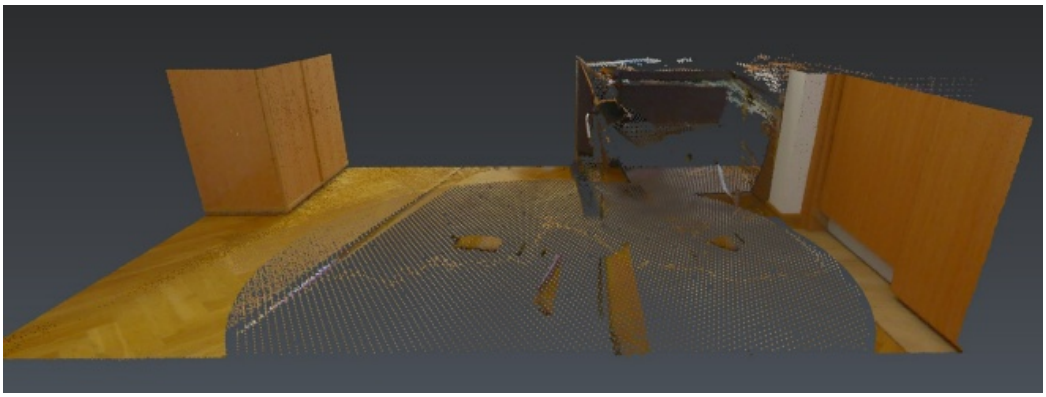

(a)

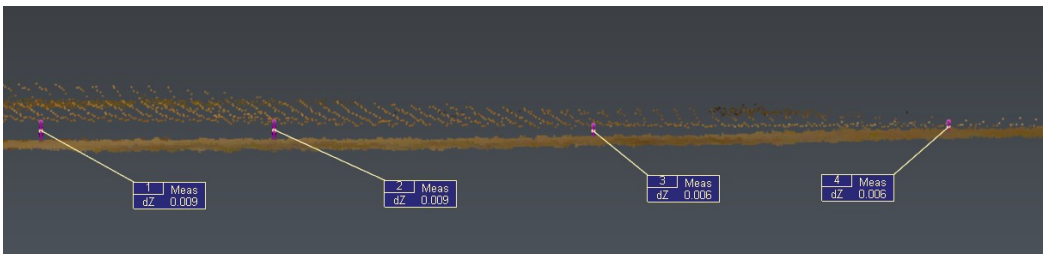

(b)

Figure 10. BLK+iPad point cloud: (a) combined point cloud beneath the first scanner position showing contrasting point densities; (b) flatness deviations for the tablet-acquired points

(a)

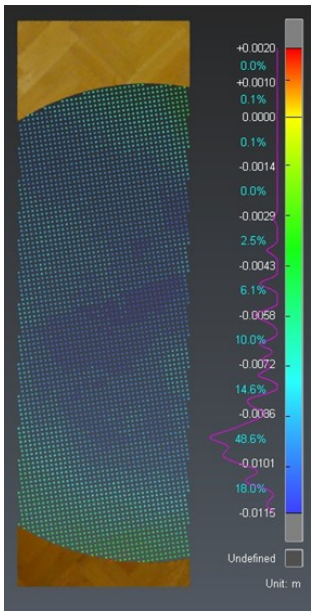

(b)

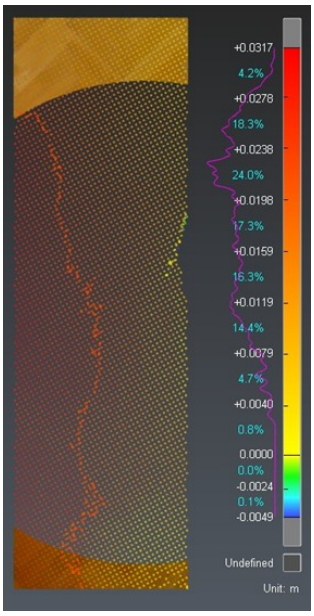

(c)

Figure 11. BLK+iPad point cloud beneath the second scanner position: (a) the two-layer structure in the filled region; (b) flatness deviations for the lower layer; (c) flatness deviations for the upper layer

References

Abbas, S. F. and Abed, F. M. (2024). *Evaluating the Accuracy of iPhone Lidar Sensor for Building Facades Conservation*, page 141–144. Springer Nature Switzerland, doi:10.1007/978-3-031-48715-6_31.

Atencio, E., Muñoz, A., Lozano, F., González-Arteaga, J., and Lozano-Galant, J. A. (2024). Calibration of iPad Pro LiDAR Scanning Parameters for the Scanning of Heritage Structures Using Orthogonal Arrays. *Applied Sciences*, 14(24):11814, doi:10.3390/app142411814.

Caffarri, C., Chirico, S., and De Falco, A. (2025). *The Use of iPad Pro's Built-in LiDAR Sensor in the Scan-to-BIM Workflow for Cultural Heritage Buildings Digitization*, page 302–316. Springer Nature Switzerland, doi:10.1007/978-3-031-98379-5_23.

Clini, P., Angeloni, R., D'Alessio, M., Coppetta, L., and Galli, I. (2025). Digital Representation and AI-driven Virtual Experience for Historic Houses. The Case Study of Borgo Storico Seghetti Panichi. *The International Archives of the Photogrammetry, Remote Sensing and Spatial Information Sciences*, XLVIII-M-9–2025:337–344, doi:10.5194/isprs-archives-xlviii-m-9-2025-337-2025.

Construction Law (1994). Act of 7 July 1994 – Construction Law. Act. Journal of Laws, 2025, item 418, Poland.

Feng, Y., Zhang, X.-L., Feng, S.-J., Zhao, Y., Kong, Q.-Z., and Zhu, S.-L. (2025). Metro tunnel deformation detection based on laser scanning robot and point cloud semantic segmentation. *Tunnelling and Underground Space Technology*, 166:106966, doi:10.1016/j.tust.2025.106966.

Fretes, H., Gomez-Redondo, M., Paiva, E., Rodas, J., and Gregor, R. (2019). A Review of Existing Evaluation Methods for Point Clouds Quality. In *2019 Workshop on Research, Education and Development of Unmanned Aerial Systems (RED UAS)*, page 247–252. IEEE, doi:10.1109/reduas47371.2019.8999725.

Gollob, C., Ritter, T., Kraßnitzer, R., Tockner, A., and Nothdurft, A. (2021). Measurement of Forest Inventory Parameters with Apple iPad Pro and Integrated LiDAR Technology. *Remote Sensing*, 13(16):3129, doi:10.3390/rs13163129.

Guerriero, L., Annibali Corona, M., Di Martire, D., Francioni, M.,

Limongiello, M., Tufano, R., and Calcaterra, D. (2024). Rockfall susceptibility analysis of the "San Michele Arcangelo" historic trail (Central Italy) based on virtual outcrops and multiple propagation models. *Bulletin of Engineering Geology and the Environment*, 83(7), doi:10.1007/s10064-024-03764-0.

Javaheri, A., Brites, C., Pereira, F., and Ascenso, J. (2017). Subjective and objective quality evaluation of 3D point cloud denoising algorithms. In *2017 IEEE International Conference on Multimedia & Expo Workshops (ICMEW)*, page 1–6. IEEE, doi:10.1109/icmew.2017.8026263.

Kottner, S., Thali, M. J., and Gascho, D. (2023). Using the iPhone's LiDAR technology to capture 3D forensic data at crime and crash scenes. *Forensic Imaging*, 32:200535, doi:10.1016/j.fri.2023.200535.

Krausková, D., Mikita, T., Hrůza, P., and Kudrnová, B. (2025). Accuracy Assessment of iPhone LiDAR for Mapping Streambeds and Small Water Structures in Forested Terrain. *Sensors*, 25(19):6141, doi:10.3390/s25196141.

Martinenko, A., Pejić, M., Obradović, M., and Ristić, N. D. (2025). Advancing 3D reconstruction: Evaluating surveying techniques for medium-sized heritage objects. *Measurement*, 256:118596, doi:10.1016/j.measurement.2025.118596.

Mokroš, M., Mikita, T., Singh, A., Tomaštík, J., Chudá, J., Wężyk, P., Kuželka, K., Surový, P., Klimánek, M., Zięba-Kulawik, K., Bobrowski, R., and Liang, X. (2021). Novel low-cost mobile mapping systems for forest inventories as terrestrial laser scanning alternatives. *International Journal of Applied Earth Observation and Geoinformation*, 104:102512, doi:10.1016/j.jag.2021.102512.

Muszyński, Z. and Rybak, J. (2021). Application of Geodetic Measuring Methods for Reliable Evaluation of Static Load Test Results of Foundation Piles. *Remote Sensing*, 13(16):3082, doi:10.3390/rs13163082.

Mêda, P., Calvetti, D., and Sousa, H. (2023). Exploring the Potential of iPad-LiDAR Technology for Building Renovation Diagnosis: A Case Study. *Buildings*, 13(2):456, doi:10.3390/buildings13020456.

Ordóñez, C., Calvopiña, J., Toapanta, S., Carranco, A., and González, J. (2024). Integrating lidar technology in artisanal and small-scale mining: A comparative study of iPad Pro LiDAR sensor and traditional surveying methods in Ecuador's artisanal gold mine. *Journal of Geodetic Science*, 14(1), doi:10.1515/jogs-2022-0181.

PN-ISO 9836:2022-07 (2022). PN-ISO 9836:2022-07: Performance standards in building – Calculation of area and volume (in Polish).

Riquelme, A., Tomás, R., Cano, M., Pastor, J. L., and Jordá-Bordehore, L. (2021). Extraction of discontinuity sets of rocky slopes using iPhone-12 derived 3DPC and comparison to TLS and SfM datasets. *IOP Conference Series: Earth and Environmental Science*, 833(1):012056, doi:10.1088/1755-1315/833/1/012056.

Rizali, M. I., Idris, A. N., Rizali, M. H., and Syafuan, W. M. (2022). Quality Assessment of 3D Point Clouds on the Different Surface Materials Generated from iPhone LiDAR Sensor. *International Journal of Geoinformatics*, page 51–59, doi:10.52939/ijg.v18i4.2259.

Saptari, A. Y., Widyastuti, R., Suhari, K. T., Suseno, A. D., Hernandi, A., Haris, R. A., and Nurmaulia, S. L. (2024). The Use of iPad LiDAR to Build a Digital Elevation Model in Defining Customary Zones (Case Study of Panglipuran, Bali). *The International Archives of the Photogrammetry, Remote Sensing and Spatial Information Sciences*, XLVIII-2/W8-2024:411–418, doi:10.5194/isprs-archives-xlviii-2-w8-2024-411-2024.

Sirmacek, B. and Lindenbergh, R. (2014). Accuracy assessment of building point clouds automatically generated from iphone images. *The International Archives of the Photogrammetry, Remote Sensing and Spatial Information Sciences*, XL–5:547–552, doi:10.5194/isprsarchives-xl-5-547-2014.

Tatsumi, S., Yamaguchi, K., and Furuya, N. (2022). ForestScanner: A mobile application for measuring and mapping trees with <scp>LiDAR</scp> -equipped <scp>iPhone</scp> and <scp>iPad</scp>. *Methods in Ecology and Evolution*, 14(7):1603–1609, doi:10.1111/2041-210x.13900.

Teppati Losè, L., Spreafico, A., Chiabrando, F., and Giulio Tonolo, F. (2022). Apple LiDAR Sensor for 3D Surveying: Tests and Results in the Cultural Heritage Domain. *Remote Sensing*, 14(17):4157, doi:10.3390/rs14174157.

Ulvi, A. and Hamal, S. N. G. (2025). Fusion of IPAD Pro LiDAR and SfM-Based Photogrammetry for 3D Documentation of Cultural Heritage. *Iranian Journal of Science and Technology, Transactions of Civil Engineering*, doi:10.1007/s40996-025-01936-w.

Vogt, M., Rips, A., and Emmelmann, C. (2021). Comparison of iPad Pro®'s LiDAR and TrueDepth Capabilities with an Industrial 3D Scanning Solution. *Technologies*, 9(2):25, doi:10.3390/technologies9020025.

Wyjadłowski, M., Muszyński, Z., and Kujawa, P. (2021). Application of Laser Scanning to Assess the Roughness of the Diaphragm Wall for the Estimation of Earth Pressure. *Sensors*, 21(21):7275, doi:10.3390/s21217275.

Zaczek-Peplinska, J. and Kowalska, M. E. (2022). Evaluation of the LiDAR in the Apple iPhone 13 Pro for use in Inventory Work. *FIG Peer Review Journal*, pages 1–19.

Zhuang, Z., Zhi, Z., Han, T., Chen, Y., Chen, J., Wang, C., Cheng, M., Zhang, X., Qin, N., and Ma, L. (2024). A Survey of Point Cloud Completion. *IEEE Journal of Selected Topics in Applied Earth Observations and Remote Sensing*, 17:5691–5711, doi:10.1109/jstars.2024.3362476.